멤브레인(Membrane Journal)
Vol. 31 No. 6 December, 2021, 417-425

Print ISSN: 1226-0088
Online ISSN: 2288-7253
DOI: https://doi.org/10.14579/MEMBRANE_JOURNAL.2021.31.6.417

# PVdF-HFP/$TiO_2$ 나노복합체 보호층을 통한 리튬금속전지 음극의 전기화학적 성능 향상

이 상 현*·최 상 석*·김 동 언*·현 준 혁*·박 용 욱*·유 진 성*·전 소 윤*·
박 중 원*·신 원 호**·손 희 상*,†

광운대학교 화학공학과
(2021년 11월 29일 접수, 2021년 11월 29일 수정, 2021년 12월 2일 채택)

# Nanostructured PVdF-HFP/$TiO_2$ Composite as Protective Layer on Lithium Metal Battery Anode with Enhanced Electrochemical Performance

**Sanghyun Lee*, Sang-Seok Choi*, Jun-Heock Hyun*, Dong-Eun Kim*, Young-Wook Park*, Jin-Seong Yu*, So-Yoon Jeon*, Joongwon Park*, Weon Ho Shin**, and Hiesang Sohn*,†**

Department of Chemical Engineering, Kwangwoon University, Seoul 01897, Republic of Korea
*(Received November 29, 2021, Revised November 29, 2021, Accepted December 2, 2021)*

요 약: 고용량 배터리에 대한 요구가 증가에 따라 기존 음극재보다 높은 용량(3,860 mAh/g)과 낮은 전기화학적 전위(-3.040 V)를 갖는 리튬 금속 기반 음극재에 대한 연구가 활발하게 이루어지고 있다. 본 연구에서는 수열 합성을 통해 제작된 아나타제(anatase) 타입의 $TiO_2$ 나노 입자 기반한 PVdF-HFP/$TiO_2$ 복합체를 리튬 금속 음극의 계면 보호층으로 적용하였다. 결정구조 및 형상 분석을 통해 유/무기-리튬 나노복합체 박막의 형성을 확인하였다. 또한, 전지화학 테스트(사이클 테스트 및 전압 프로파일)를 통해 리튬 금속 음극의 전기화학 성능 은 복합체 보호막이 $TiO_2$ 10 wt%, 코팅 두께 1.1 μm의 조건에서 가장 개선된 전기화학적 성능(콜롱 효율 유지: 77 사이클 동안 90% 이상) 발현을 확인하였다. 이를 통해, 처리하지 않은 리튬 전극 대비 본 보호층에 의한 리튬 금속 음극의 성능 안정화/개선 효과가 검증되었다.

**Abstract:** As the demand for high-capacity batteries increases, there has been growing researches on the lithium metal anode with a capacity (3,860 mAh/g) of higher than that of conventional one and a low electrochemical potential (-3.040 V). In this study, using the anatase phased $TiO_2$ nanoparticles synthesized by hydrothermal synthesis, a PVdF-HFP/$TiO_2$ organic/inorganic composite material was designed and used as an interfacial protective layer for a Li metal anode. As-formed organic/inorganic-lithium composite thin film was confirmed through the crystalline structure and morphological analyses. In addition, the electrochemical test (cycle stability and voltage profile) confirmed that the protective layer of PVdF-HFP/$TiO_2$ composite (10 wt% $TiO_2$ and 1.1 μm film thickness) contributed to the enhanced electrochemical performance of the lithium metal anode (Colombic efficiency retention: 90% for 77 cycles). Based on comparative test with the untreated lithium electrode, it was confirmed that our protective layer plays an important role to stabilize/improve the EC performance of the lithium metal negative electrode.

***Keywords:*** *Li metal battery (LMB), $TiO_2$ nanoparticle, hydrothermal synthesis, protective layer, PVdF-HFP*

## 1. Introduction

In recent years, it is essential to equip electronic devices and electric vehicles with a high performance lithium-ion battery (LIB) having a high energy density and a high-capacity[1-3]. However, due to the insufficient energy density of current LIB, it is required to develop the new electrode material for the development of high performance LIBs. Specifically, conventional LIB exhibit limited electrochemical (EC) per-

†Corresponding author(e-mail: sonisang@hanmail.net; http://orcid.org/0000-0002-4164-9397)

formances due to low capacity (372 mAh/g) of graphite based anode. In this context, there have been many attempts made to replace the previously used graphite based anode with novel materials having a higher capacity such as Si, Sn, metal oxides and lithium[4-15]. Among them, lithium metal anode based LIB, or lithium metal batteries (LMB), are very attractive due to their high theoretical capacity (3,860 mAh/g) and the lowest electrochemical potential (−3.040 V vs. standard hydrogen electrode)[16-19].

Despite aforementioned advantages, LMBs have been struggled to be commercialized owing to low EC performance (low coulombic efficiency (CE) and low cycle stability), and safety issues. More specifically, a higher electric field is formed around the tip of lithium metal anode in the LMB during lithium electrodeposition, resulting in the formation of vertically grown lithium dendrites by the intensively electrodeposited lithium on the tip[20-22]. As-formed dendrites adheres to the surface of the lithium metal, making non-uniform anode surface. Then, the as-grown dendrite pass through the solid-electrolyte interface (SEI) followed by separator penetration, leading to fire explosion, swollen electrode and short circuit of the electrodes. In addition, during the discharges, eluted lithium from the dendrites forms electrically short-circuited 'dead' lithium, alleviating the coulombic efficiency. After repeated processes, porous layers are formed and accumulated on the lithium metal anode surface by reaction with electrolyte, accelerating the inhomogeneous electrode reaction by the increased electrode resistance as well as shortening the battery life of LMB[23-30]. It is required to address the formation of lithium dendrite for the improved EC performance of LMB.

In this study, we demonstrated a novel approach to enhance the EC performance of LMB by deposition of PVdF-HFP/$TiO_2$ nanocomposite based protective layer on lithium metal anode. Based on the hypothesis of organic/inorganic nanostructure based protective layer can effectively suppress the lithium dendrite formation by cooperative function of PVdF-HFP with excellent physical/chemical stability and $TiO_2$ nanoparticles with enhanced mechanical flexibility, we prepared the organic (PVdF-HFP) and inorganic ($TiO_2$) nanocomposite and analysed with structural (XRD), morphological (TEM and SEM) and electrochemical characterizations[31-34].

We believe current approach will be conducive to address the current issues of lithium metal batteries, allowing to be applied practical battery application with enhanced energy density and capacity.

## 2. Experimental section

### 2.1. Materials

Tert-butylamine (Duksan, Extra pure), oleic acid (OA, Daejung, Extra pure), toluene (Samchun, 99.5%), and titanium (IV) iso-propoxide [TTIP, (Ti($OPr_2$)), Sigma-Aldrich, 97%], polyvinlyidene fluoride-co-hexafluoropropylene (PVdF-HFP, Sigma-Aldrich) and N-methyl-2-pyrrolidone (NMP, Sigma-Aldrich) were used as-received without further purification.

### 2.2. Synthesis of PVdF-HFP/$TiO_2$ nanocomposite thin film

#### 2.2.1. $TiO_2$ nanoparticles

$TiO_2$ nanoparticles were prepared by two-phase interfacial reaction through hydrothermal process. Briefly, 3 g of TTIP were mixed with 10 g of oleic acid in the 50 mL of toluene followed by added with 10 mL of DI-water containing 0.1 mL of tert-butylamine. As-prepared solution were transferred to autoclave and keep it at at 180°C for 10 hours. In this process, yellow solution of $TiO_2$ nanoparticles stabilized with oleic acid were synthesized, exhibiting reverse micelle structure. After reaction, white $TiO_2$ nanopaticles can be obtained by precipitation through methanol mixing and centrifuge.

#### 2.2.2. PVdF-HFP/$TiO_2$ nanocomposite thin film

The nanocomposite of PVdF-HFP/$TiO_2$ were prepared by mixing $TiO_2$ nanoparticles with PVdF-HFP solution followed by film deposition. For instance, a coating solution of PVdF-HFP/$TiO_2$ composite was prepared by mixing 5~10% of $TiO_2$ nanoparticle sol-

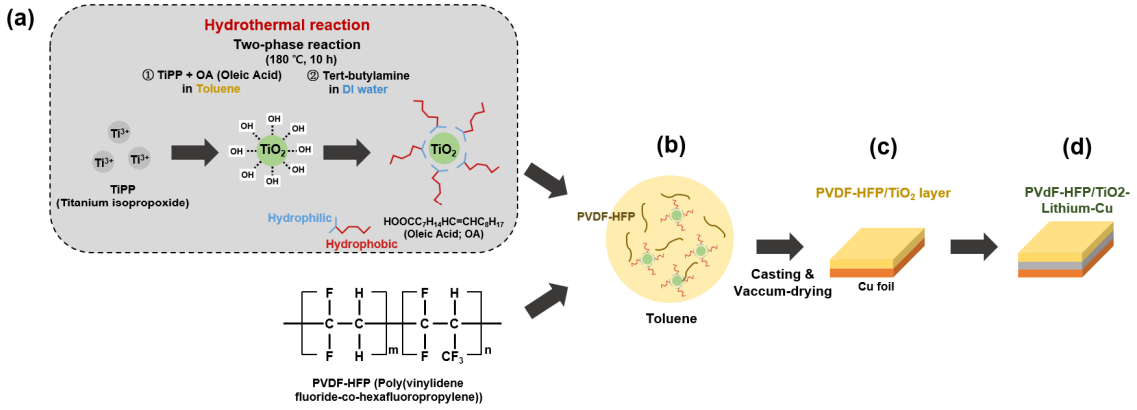


**Scheme 1.** Fabrication process of PVdF-HFP/$TiO_2$ composite based protective layer on lithium metal electrode. (a) $TiO_2$ synthesis (b) PVdF-HFP/$TiO_2$ composite preparation (c) Composite protective layer preparation (d) PVdF-HFP/$TiO_2$ composite on lithium metal electrode.

ution in toluene with 0.5 g of PVdF-HFP in NMP. The coating solution was deposited on copper (Cu) substrate with doctor blade coating with a thickness of 30~100 μm. The as-coated Cu foil with a composite of PVdF-HFP/$TiO_2$ was dried in a vacuum oven at 60°C for 24 hours.

### 2.3. Material characterization

The morphologies of $TiO_2$ nanoparticles was observed through the transmission electron microscopy (TEM) and high-resolution TEM (HR-TEM, JEOL/CEOS, JEM-2100F, Cs collector). The surface and cross-sectional morphology of the PVdF-HFP/$TiO_2$ thin film was observed with scanning electron microscopy (SEM, Hitachi, S-4300SE). In addition, the element composition and distribution of PVdF-HFP/$TiO_2$ composite film was obtained SEM equipped with energy dispersive X-ray spectroscopy (EDS). The crystalline structure of $TiO_2$ nanoparticles and PVdF-HFP/$TiO_2$ composite were investigated by X-ray diffraction (XRD, Rigaku, D/Max-2500) in the $2\theta$ range of 20~80° using Cu-K$\alpha$ radiation.

### 2.4. Electrochemical characterization

For electrochemical characterization, CR-2032-Type coin cell was fabricated. Bare Cu or protective layers (PVdF-HFP or PVdF-HFP/$TiO_2$) treated Cu were employed as a working electrode while Li foil was applied as a counter electrode. 1 M LiTFSI was used for DOL(1,3-Dioxolane)/DME(1,2-Dimethoxyethane) (1:1 = v:v) as the electrolyte while polyethylene membrane (Celgard 2400) was used as the separator. Coin cells were prepared in a glove box filled with Ar gas. Coulomb efficiency and voltage profile are measured with a battery tester (WBCS 3000, Wonatech). All cells were subjected to precycling to induce lithium deposition before the test. The initial cycle for precycling was performed under plating rate of 3 mAh/$cm^2$ at a current density of 0.1 mA/$cm^2$ while the stripping was carried out up to 1.2 V. Coulombic efficiency was measured by stripping up to 1.2 V after lithium plating with a capacity of 1 mAh/$cm^2$ at 1 mA/$cm^2$. The overpotential was confirmed through the cycle-by-cycle voltage profile analyses.

## 3. Results and discussion

### 3.1. Material analyses

As displayed in the schematic fabrication process of PVdF-HFP/$TiO_2$ composite thin film(Scheme 1), the composite layer were synthesized by sequential hydrothermal process for $TiO_2$ nanoparticles synthesis[scheme 1(a)] followed by composite formation [scheme 1(b)] and composite thin film deposition [scheme 1(c)]. The synthesis of anatase phased $TiO_2$ nanoparticles[scheme 1(a)] were carried out through a two-phase reaction

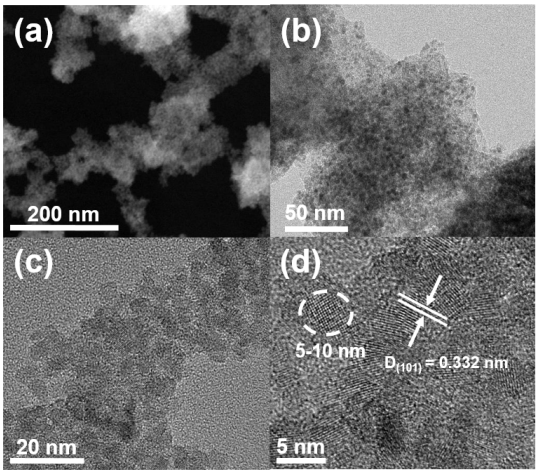


**Fig. 1.** (a) TEM and high resolution TEM images for $TiO_2$ nanoparticles obtained at various magnifications (a) 20.0 k, (b) 100.0 k, (c) 200.0 k, (d) 800.0 k.

hydrothermal process (180°C, 10 h) to enhance the dispersibility in polymer matrix (PVdF-HFP). In contrast to the conventional aqueous phase-based $TiO_2$ synthesis with limited application towards organic/inorganic composite due to its poor dispersibility (aggregation) in organic solvent or polymer, our $TiO_2$ nanoparticles stabilized with oleic acid shows the high dispersibility in hydrophobic solvents, leading to good compatibility in the PVdF-HFP based composite solution[scheme 1(b)]. As-prepared composite solution was coated on Cu foil and dried in the vacuum oven at 60°C for 24 hours to obtain an a PVdF-HFP/$TiO_2$ on Cu foil without $TiO_2$ aggregation in the composite film[scheme 1(c)]. In the end, the composite film on Cu was further electrochemically lithiated to have a structure of PVdF-HFP/$TiO_2$-Lithium-Cu foil[scheme 1(d)].

Fig. 1 displays the nanomorphology of as-synthesized $TiO_2$ nanoparticle obtained by high-resolution transmission electron microscopy (HR-TEM). Figs. 1(a) and 1(b) display $TiO_2$ nanoparticles imaged at 20.0 k and 100.0 k magnification, respectively. The nanomophormlogy of $TiO_2$ nanoparticle confirmed the maintained spherical shape without aggregation. Fig. 1(c) displays the enlarged TEM image of $TiO_2$ nanoparticles with uniform size distribution (5~10 nm). As displayed in Fig. 1(d), the crystal direction of $TiO_2$

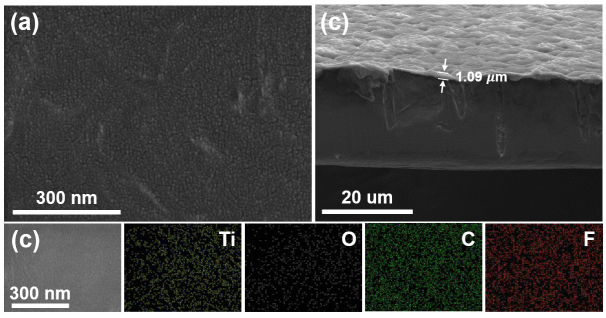


**Fig. 2.** SEM images of PVdF-HFP/$TiO_2$ layer on (a) top-view, (b) cross-section. (c) EDS maps of protective layer (Ti (yellow), O (white), C (green), F (red)).

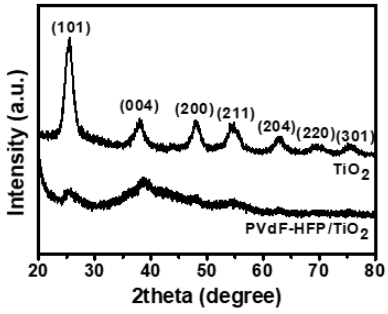


**Fig. 3.** X-ray diffraction (XRD) analyses on the $TiO_2$ nanoparticle and PVdF-HFP/$TiO_2$ composites.

nanoparticle was identified as (101) with the inter-crystal distance of 0.332 nm, indicating the formation of anatase crystalline phase of $TiO_2$ nanoparticles.

Fig. 2 display the surface and cross-sectional morphology of PVdF-HFP/$TiO_2$ composite film deposited on Cu current collector obtained by SEM. The SEM image (plane view) for the protective PVdF-HFP/$TiO_2$ composite film[Fig. 2(a)], displays the uniform distribution of $TiO_2$ nanoparticles without agglomeration. As displayed in the cross-sectional morphology of PVdF-HFP/$TiO_2$ nanocomposite film[Fig. 2(b)], the film thickness is estimated as 1.1, 1.2, and 3.1 μm, respectively after solvent evaporation of coating solution under vacuum (coating thickness before drying: 30, 70, 100 μm). Fig. 2(c) is an elemental mapping [titanium (Ti: yellow), oxygen (O: white), carbon (C: green), fluorine (F: red))] image of the protective layer obtained with SEM-EDS, confirming the homogeneous distribution of $TiO_2$ throughout the PVdF-HFP matrix.

Fig. 3 displays the crystalline structure of $TiO_2$ nanoparticle embedded int's polymer to form $TiO_2$-PVdF/$TiO_2$ composite. The (101) is a characteristic XRD peak of anatase-phased $TiO_2$ located at peak 25.3°. In addition, the peaks of (004), (200), (211), and (204) further confirms the synthesis of anatase phased $TiO_2$ nanoparticles[35-38]. In the semi-crystalline polymer displays a broad peak at 20.0° and 38.8°[39]. Thus, the XRD result suggests the formation of anatase-phased $TiO_2$ nanoparticle and PVdF-HFP/$TiO_2$ composite with good compatability each other and without any noticeable phase change of the $TiO_2$ nanoparticles in the composite.

### 3.3. Electrochemical analyses

The EC characterization for the pristine lithium (bare Cu electrode) and lithium protected with composite layers (PVdF-HFP, PVdF-HFP/$TiO_2$) were compared to investigate the effect of protective layer on EC performance. Fig. 4(a) compares the couloumbic efficiencies (CEs) of samples measured at the current density of 1 mA/$cm^2$. The CE of lithium anode formed on bare Cu decreased over 20% at the 23$^{rd}$ cycle. The CE of PVdF-HFP on lithium anode decreased to less than 80% in the 37$^{th}$ cycle was used as a protective layer. However, the lithium anode treated with protective layer of PVdF-HFP/$TiO_2$ 10 wt% exhibited a excellent CE retention of over 80% until 77 cycles, confirming the improved EC performance by application of our PVdF-HFP/$TiO_2$ composite layer on lithium. Fig. 4b displays the coulombic efficiency of lithium anode protected with layer of PVdF-HFP/$TiO_2$ composites ($TiO_2$: 0, 5, 10 wt%) measured at a current density of 2 mA/$cm^2$. The lithium anode treated with composite protective layers containing low $TiO_2$ (0 wt% and 5 wt%) display very unstable coulombic efficiency at elongated cycles under high current density (2 mA/$cm^2$). In contrast, the Coulombic efficiency of lithium protected with our composite with optimal $TiO_2$ nanoparticles (5 wt%) showed a very stable coulombic efficiency of around 80% until the 33 cycles under identical condition. Figs. 4c-d compare the voltage profile in the initial cycle[Fig. 4(b)] and the 100$^{th}$ cycle[Fig. 4(c)] of samples (bare Cu, PVdF-HFP, PVdF-HFP/$TiO_2$). In the initial voltage profile[Fig. 4(b)], although PVdF-HFP/$TiO_2$ based protective layer showed larger overpotential than that of Cu foil, the difference is not significantly large. However, in the voltage profile after 100$^{th}$ cycle, PVdF-HFP/$TiO_2$ protective layer treated one exhibited negligible overpotential change whereas that of bare Cu and PVdF-HFP displays significantly increased.

As described, the lithium anode treated with our composite (PVdF-HFP/$TiO_2$) exhibited superior performance to those with controls (untreated and PVdF-HFP/$TiO_2$ with low $TiO_2$ contents). Such an application of a composited protective layer of semi-crystalline polymer (PVdF-HFP) and anatase-phased $TiO_2$ with high ionic conductivity and high mechanical properties allows the interfacial stabilization (inhibited dendrite growth), leading to the enhanced EC performance (retained coulombic efficiency at elongated cycles) [34,40].

Scheme 2 compares the mechanism of plating/stripping of lithium on bare Cu[Scheme 2(a)] and PVdF-HFP/$TiO_2$ composite treated one [Scheme 2(b)] during the lithiation/delithiation. As shown in Scheme 2(a), nonuniform lithium nuclei and subsequent layer formed on the bare Cu at the initial and subsequent plating (lithiation). Then, lithium ion flux is concentrated on the non-uniform nuclei followed by the formation/growth of lithium dendrites[41,42]. During stripping, nonuniform lithium layer results in the formation of electrically inactive lithium (dead lithium), leading to continuous drop in the CE and overpotential. On the other hand, as illustrated in Scheme 2(b), PVdF-HFP/$TiO_2$ composite protective layer deposited electrode induce homogeneous formation of lithium nuclei (lithium ion flux) and horizontal plating of lithium due to high ionic conductivity and mechanical robustness of composite layer[27-30]. During the stripping (delithiation), the protective layer prevent direct contact of lithium from the electrolyte to reduce the electrolyte decomposition, leading to suppressed formation of inactive lithium formation. Thus, the lithium debris on electrode can be effectively removed at a high rate, leading to retained CE and reduced overpotential[43].

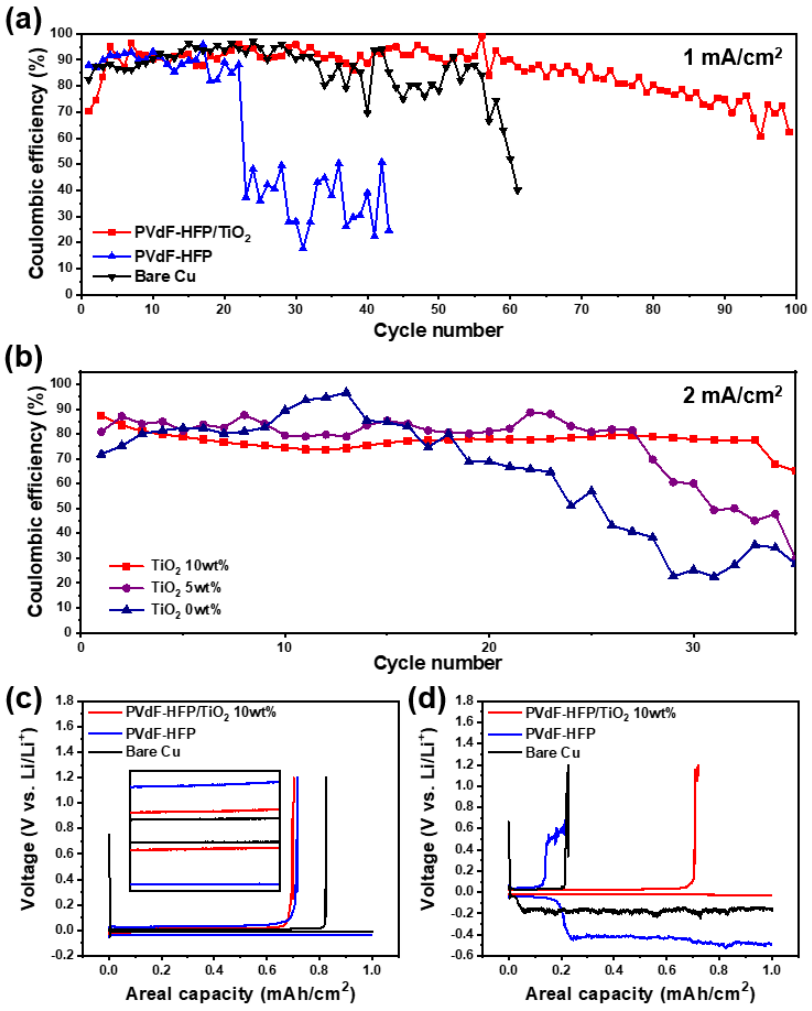


**Fig. 4.** Electrochemical analysis of bare Cu (untreated one), PVdF-HFP, PVdF-HFP/$TiO_2$-coated electrode. (a) Coulombic efficiency at 1 mA/$cm^2$, (b) Coulombic efficiency according to $TiO_2$ content at 2 mA/$cm^2$, (c) Voltage profiles at initial cycle, (d) Voltage profiles at $100^{th}$ cycle.

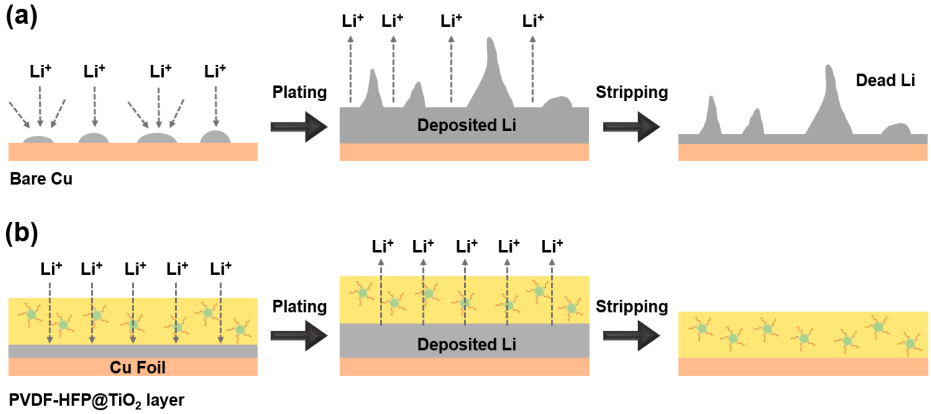


**Scheme 2.** Schematic illustration of Li plating/stripping behavior (a) bare lithium metal anode, (b) PVdF-HFP/$TiO_2$ composite protective layer on lithium metal.

## 4. Conclusions

In this work, we demonstrated a PVdF-HFP/$TiO_2$ nanocomposite as a protective layer to be applied on a lithium-metal battery anode. We successfully synthesized $TiO_2$ nanoparticles through two-phase hydrothermal process. In the morphological analyses by TEM, it was confirmed to synthesize anatase phased $TiO_2$ nanoparticles with a size of 5~10 nm in a crystal direction of (101) and an inter-crystal distance of 0.332 nm. The composite film morphology obtained by SEM exhibit good compatibility of $TiO_2$ nanoparitcles with PVdF-HFP matrix, resulting in the formation of a PVdF-HFP/$TiO_2$ composite without aggregations.

EC characterization exhibited the superior performance of lithium metal anode by application of PVdF-HFP/$TiO_2$ composite to controls (lithium anode treated with PVdF-HFP and non-treated). In the cycle performance and voltage profile test, the CE of lithium anode protected with PVdF-HFP/$TiO_2$ composite thin film was greater than 90% for 77 cycles and no-significant profile change was observed whereas the controls did not.

As demonstrated in this work, the good compatibility of organic (PVdF-HFP) and inorganic ($TiO_2$) in the composite protective layer plays an important role to induce uniform nucleation and horizontal electrodeposition of lithium, leading to enhanced EC performance. We believe this work will be important corner stone for the forthcoming study on the stabilization of interface between lithium and protective layer.

## Acknowledgements

The present research has been conducted by the Research Grant of Kwangwoon University in 2020. This research was supported by the Nano-Material Technology Development Program through the National Research Foundation of Korea (NRF), funded by the Ministry of Science, ICT and Future Planning (2009-0082580). It was also supported by an NRF grant funded by the Korean government (MSIT) (No. NRF-2020R1F1A1065536) and by Korea Institute for Advancement of Technology (KIAT) grant funded by the Korea Government (MOTIE) (P0012451, The Competency Development Program for Industy Specialist).

## Reference

1. B. A. Korgel, “Nanomaterials developments for higher-performance lithium ion batteries”, *J. Phys. Chem. Lett.*, **5**, 749 (2014).
2. L. Yue, J. Ma, J. Zhang, J. Zhao, S. Dong, Z. Liu, G. Cui, and L. Chen, “All solid-state polymer electrolytes for high-performance lithium ion batteries”, *Energy Storage Mater.*, **5**, 139 (2016).
3. A. Eftekhari, “Lithium batteries for electric vehicles: From economy to research strategy”, *ACS Sustain. Chem. Eng.*, **7**, 5602 (2019).
4. D. Seok, Y. Jeong, K. Han, D. Y. Yoon, and H. Sohn, “Recent progress of electrochemical energy devices: Metal oxide–carbon nanocomposites as materials for next-generation chemical storage for renewable energy”, *Sustainability*, **11**, 3694 (2019).
5. H. Jung, M. Park, Y.-G. Yoon, G.-B. Kim, and S.-K. Joo, “Amorphous silicon anode for lithium-ion rechargeable batteries”, *J. Power Sources*, **115**, 346 (2003).
6. J. Xiao, W. Xu, D. Wang, D. Choi, W. Wang, X. Li, G. L. Graff, J. Liu, and J.-G. Zhang, “Stabilization of silicon anode for Li-ion batteries”, *J. Electrochem. Soc.*, **157**, A1047 (2010).
7. G. Huang, J. Han, Z. Lu, D. Wei, H. Kashani, K. Watanabe, and M. Chen, “Ultrastable silicon anode by three-dimensional nanoarchitecture design”, *ACS Nano*, **14**, 4374 (2020).
8. K. Hwang, N. Kim, Y. Jeong, H. Sohn, and S. Yoo, “Controlled nanostructure of a graphene nanosheet-$TiO_2$ composite fabricated via mediation of organic ligands for high-performance Li storage applications”, *Int. J. Energy Res.*, **45**, 16189 (2021).
9. D. Seok, W. H. Shin, S. W. Kang, and H. Sohn, “Piezoelectric composite of $BaTiO_3$-coated $SnO_2$ microsphere: Li-ion battery anode with enhanced

electrochemical performance based on accelerated $Li^+$ mobility", *J. Alloys Compd.*, **870**, 159267 (2021).
10. H. Ota, K. Shima, M. Ue, and J.-i. Yamaki, "Effect of vinylene carbonate as additive to electrolyte for lithium metal anode", *Electrochim. Acta*, **49**, 565 (2004).
11. F. Dai, R. Yi, H. Yang, Y. Zhao, L. Luo, M. L. Gordin, H. Sohn, S. Chen, C. Wang, S. Zhang, and D. Wang, "Minimized volume expansion in hierarchical porous silicon upon lithiation", *ACS Appl. Mater. Interfaces*, **11**, 13257 (2019).
12. K. Hwang, H. Sohn, and S. Yoon, "Mesostructured niobium-doped titanium oxide-carbon (Nb-$TiO_2$-C) composite as an anode for high-performance lithium-ion batteries", *J. Power Sources*, **378**, 225 (2018).
13. H. Sohn, D. H. Kim, R. Yi, D. Tang, S.-E. Lee, Y. S. Jung, and D. Wang, "Semimicro-size agglomerate structured silicon-carbon composite as an anode material for high performance lithium-ion batteries", *J. Power Sources*, 334, 128 (2016).
14. H. Sohn, Z. Chen, Y. S. Jung, Q. Xiao, M. Cai, H. Wang, and Y. Lu, "Robust lithium-ion anodes based on nanocomposites of iron oxide-carbon-silicate", *J. Mater. Chem. A*, **1**, 4539 (2013).
15. Y. Jeong, J. Park, S. Lee, S. H. Oh, W. J. Kim, Y. J. Ji, G. Y. Park, D. Seok, W. H. Shin, J.-M. Oh, T. Lee, C. Park, A. Seubsai, and H. Sohn, "Iron oxide-carbon nanocomposites modified by organic ligands: Novel pore structure design of anode materials for lithium-ion batteries", *J. Elec. Anal. Chem*., **904**, 115905 (2022).
16. B. Liu, J.-G. Zhang, and W. Xu, "Advancing lithium metal batteries", *Joule*, **2**, 833 (2018).
17. S. Park, H.-J. Jin, and Y. S. Yun, "Advances in the design of 3D-structured electrode materials for lithium-metal anodes", *Adv. Mater.*, **32**, 2002193 (2020).
18. H. Sohn, "Deposition of functional organic and inorganic layer on the cathode for the improved electrochemical performance of Li-S battery", *Korean Chem. Eng. Res.*, **55**, 483 (2017).
19. H. Sohn, M. L. Gordin, M. Regula, D. H. Kim, Y. S. Jung, J. Song, and D. Wang, "Porous spherical polyacryonitrile-carbon nanocomposite with high loading of sulfur for lithium-sulfur batteries", *J. Power Sources*, **302**, 70 (2016).
20. F. Ding, W. Xu, G. L. Graff, J. Zhang, M. L. Sushko, X. Chen, Y. Shao, M. H. Engelhard, Z. Nie, J. Xiao, X. Liu, P. V. Sushko, J. Liu, and J.-G. Zhang, "Dendrite-free lithium deposition via self-healing electrostatic shield mechanism", *J. Am. Chem. Soc.*, **135**, 4450 (2013).
21. J. Z. Hu, Z. Zhao, M. Y. Hu, J. Feng, X. Deng, X. Chen, W.Xu, J. Liu, and J.-G. Zhang, "In situ $^7$Li and $^{133}$Cs nuclear magnetic resonance investigations on the role of $Cs^+$ additive in lithium-metal deposition process", *J. Power Sources*, **304**, 51 (2016).
22. C. Yan, X.-B. Cheng, Y. Tian, X. Chen, X.-Q. Zhang, W.-J. Li, J.-Q. Huang, and Q. Zhang, "Dual-layered film protected lithium metal anode to enable dendrite-free lithium deposition", *Adv. Mater.*, **30**, 1707629 (2018).
23. H. Liu, H. Zhou, B.-S. Lee, X. Xing, M. Gonzalez, and P. Liu, "Suppressing lithium dendrite growth with a single-component coating", *ACS Appl. Mater. Interfaces*, **9**, 30635 (2017).
24. G. Yang, J. Chen, P. Xiao, P. O. Agboola, I. Shakir, and Y. Xu, "Graphene anchored on Cu foam as a lithiophilic 3D current collector for a stable and dendrite-free lithium metal anode", *J. Mater. Chem. A*, **6**, 9899 (2018).
25. Y. Cheng, X. Ke, Y. Chen, X. Huang, Z. Shi, and Z. Guob, "Lithiophobic-lithiophilic composite architecture through co-deposition technology toward high-performance lithium metal batteries", *Nano Energy*, **63**, 103854 (2019).
26. H. Liu, X. Wang, H. Zhou, H.-D. Lim, X. Xing, Q. Yan, Y. S. Meng, and P. Liu, "Structure and solution dynamics of lithium methyl carbonate as a protective layer for lithium metal", *ACS Appl. Energy Mater.*, **1**, 1864 (2018).
27. Y. Zhong, Y. Chen, Y. Cheng, Q. Fan, H. Zhao,

H. Shao, Y. Lai, Z. Shi, X. Ke, and Z. Guo, "Li alginate-based artificial SEI layer for stable lithium metal anodes", *ACS Appl. Mater. Interfaces*, **11**, 37726 (2019).
28. S. Lee, D. Seok, Y. jeong, and H. Sohn, "Surface modification of Li metal electrode with PDMS/GO composite thin film: Controlled growth of Li layer and improved performance of lithium metal battery (LMB)", *Membr. J.*, **30**, 38 (2020).
29. W. Liu, W. Li, D. Zhuo, G. Zheng, Z. Lu, K. Liu, and Y. Cui, "Core–shell nanoparticle coating as an interfacial layer for dendrite-free lithium metal anodes", *ACS Cent. Sci.*, **3**, 135 (2017).
30. Z. Wen, Y. Peng, J. Cong, H. Hua, Y. Lin, J. Xiong, J. Zeng, and J. Zhao, "A stable artificial protective layer for high capacity dendrite-free lithium metal anode", *Nano Res*. **12**, 2535 (2019).
31. H. Xie, Z. Tang, Z. Li, Y. He, Y. Liu, and H. Wang, "PVDF-HFP composite polymer electrolyte with excellent electrochemical properties for Li-ion batteries", *J. Solid State Electrochem.*, **12**, 1497 (2008).
32. A. M. Stephan, K. S. Nahm, M. A. Kulandainathan, G. Ravi, and J. Wilson, "Poly (vinylidene fluoride-hexafluoropropylene)(PVdF-HFP) based composite electrolytes for lithium batteries", *Eur. Polym. J.*, **42**, 1728 (2006).
33. B. Zhu, Y. Jin, X. Hu, Q. Zheng, S. Zhang, Q. Wang, and J. Zhu, "Poly (dimethylsiloxane) thin film as a stable interfacial layer for high-performance lithium-metal battery anodes", *Adv. Mater.*, **29**, 1603755 (2017).
34. Y. Nan, S. Li, B. Li, and S. Yang, "An artificial $TiO_2$/lithium n-butoxide hybrid SEI layer with facilitated lithium-ion transportation ability for stable lithium anodes", *Nanoscale*, **11**, 2194 (2019).
35. X. Lü, P. Hao, G. Xie, J. Duan, L. Gao, and B. Liu, "A sensor array realized by a single flexible $TiO_2$/POMs film to contactless detection of triacetone triperoxide", *Sensors*, **19**, 915 (2019).
36. M. Xie, L. Jing, J. Zhou, J. Lin, and H. Fu, "Synthesis of nanocrystalline anatase $TiO_2$ by one-pot two-phase separated hydrolysis-solvothermal processes and its high activity for photocatalytic degradation of rhodamine B", *J. Hazard. Mater.*, **176**, 139 (2010).
37. K. Hwang, N. Kim, Y. Jeong, H. Sohn, and S. Yoon, "Controlled nanostructure of a graphene nanosheet-$TiO_2$ composite fabricated via mediation of organic ligands for high-performance Li storage applications", *Int. J. Energy Res.*, **45**, 16189 (2021).
38. H. Sohn, D. Kim, J. Lee, and S. Yoon, "Facile synthesis of a mesostructured $TiO_2$–graphitized carbon ($TiO_2$–gC) composite through the hydrothermal process and its application as the anode of lithium ion batteries", *RSC Adv.*, **6**, 39484 (2016).
39. Singh, V. Kumar, and R. K. Singh., "Development of ion conducting polymer gel electrolyte membranes based on polymer PVdF-HFP, BMIMTFSI ionic liquid and the Li-salt with improved electrical, thermal and structural properties", *J. Mater. Chem. C*, **3**, 7305 (2015).
40. M. Wang, X. Cheng, T. Cao, J. Niu, R. Wu, X. Liu, Y. Zhang, "Constructing ultrathin $TiO_2$ protection layers via atomic layer deposition for stable lithium metal anode cycling", *J. Alloys Compd.*, **865**, 158748 (2021).
41. R. Zhang, X.-R. Chen, X. Chen, X.-B. Cheng, X.-Q. Zhang, C. Yan, and Q. Zhang, "Lithiophilic sites in doped graphene guide uniform lithium nucleation for dendrite-free lithium metal anodes", *Angew. Chem., Int. Ed.*, **129**, 7872 (2017).
42. L. Pan, Z. Luo, Y. Zhang, W. Chen, Z. Zhao, Y. Li, J. Wan, D. Yu, H. He, and D. Wang, "Seed-free selective deposition of lithium metal into tough graphene framework for stable lithium metal anode", *ACS Appl. Mater. Interfaces*, **11**, 44383 (2019).
43. R. Xu, X.-Q. Zhang, X.-B. Cheng, H.-J. Peng, C.-Z. Zhao, C. Yan, and J.-Q. Huang, "Artificial soft–rigid protective layer for dendrite-free lithium metal anode", *Adv. Funct. Mater.*, **28**, 1705838 (2018).